

Article

Wind Turbine Power Maximization Using Log-Power Proportional-Integral Extremum Seeking

Devesh Kumar ¹  and Mario A. Rotea ^{2,*} 

¹ Department of Electrical and Computer Engineering and Center for Wind Energy, The University of Texas at Dallas, Richardson, TX 75080, USA; devesh.kumar@utdallas.edu

² Department of Mechanical Engineering and Center for Wind Energy, The University of Texas at Dallas, Richardson, TX 75080, USA

* Correspondence: rotea@utdallas.edu

Abstract: This paper proposes a Log-Power Proportional-Integral Extremum Seeking Control (LP-PIESC) framework for maximizing the power capture of a wind turbine operating at below-rated wind speeds, i.e., the so-called region-2 of a turbine's power curve. Extremum seeking control (ESC) has emerged as a viable algorithm to maximize energy capture for a wind turbine operating in region-2. Despite the encouraging results of early ESC strategies, the basic algorithm suffers from slow and inconsistent convergence behavior under changing wind speed within region-2. It has been shown that replacing the power signal with its logarithm results in an algorithm that is robust and predictable even when the mean wind speed varies. In addition, new studies have suggested that replacing conventional ESC with proportional plus integral ESC (PIESC) results in faster convergence to optimal conditions. In the current paper, the idea of log-power feedback is merged with the PIESC scheme and is applied to tune the parameters of the region-2 torque controller for the NREL 5-MW turbine reference model. The results of this new algorithm are compared with the ESC with log-of-power feedback using NREL OpenFAST simulations. The log-power feedback PIESC is also implemented for the blade pitch set-point angle. Energy capture over the course of the simulations and damage equivalent loads calculated with MLife are used to assess the results. The simulations performed under different turbulent intensity cases demonstrate the rapid convergence of the log-power feedback PIESC.

Keywords: wind turbine power maximization; proportional-integral extremum seeking control (PIESC); log-of-power (LP) feedback



Citation: Kumar, D.; Rotea, M.A. Wind Turbine Power Maximization Using Log-Power Proportional-Integral Extremum Seeking. *Energies* **2022**, *15*, 1004. <https://doi.org/10.3390/en15031004>

Academic Editors: Mircea Neagoe, Radu Săulescu and Codruta Jaliu

Received: 19 December 2021

Accepted: 26 January 2022

Published: 29 January 2022

Publisher's Note: MDPI stays neutral with regard to jurisdictional claims in published maps and institutional affiliations.



Copyright: © 2022 by the authors. Licensee MDPI, Basel, Switzerland. This article is an open access article distributed under the terms and conditions of the Creative Commons Attribution (CC BY) license (<https://creativecommons.org/licenses/by/4.0/>).

1. Introduction

Wind turbines extract power in two different wind regimes: above-rated wind speed when the machine is regulated to produce its rated power while maintaining the rated rotor angular speed despite wind variations, and below-rated wind speed when the angular rotor speed is actively controlled to maximize the power extracted from the wind. These two modes of operation are loosely referred to as region-3 (above-rated wind condition) and region-2 (below-rated wind conditions).

The rotor power in region-2 is proportional to the available wind power, and the proportionality parameter, i.e., the power coefficient, or aerodynamic efficiency, is optimized to maximize the output power. In variable-speed variable-pitch turbines, the power coefficient (C_p) is a unimodal function of the tip-speed ratio (λ) and the blade-pitch angle (β) [1], which implies there is an optimal tip-speed ratio and blade-pitch angle for achieving the optimal C_p and thus maximum output power. In practice, below-rated (region-2) operation entails keeping the blade-pitch angle constant at its ideal value β_{opt} while adjusting the rotor speed to maintain the optimal tip-speed ratio λ_{opt} despite wind changes [1,2]. Optimal tip-speed ratios and blade-pitch angles can differ from the manufacturer's specification due

to site-specific complex aerodynamic effects and other factors. Furthermore, the optimal settings for these turbine parameters may change over time because of the blade wear and tear, variations in environmental conditions, etc.

Extremum Seeking Control (ESC) has emerged as an effective real-time optimization strategy to maximize power capture in region-2 despite a lack of knowledge of optimal turbine parameters. The ESC is a gradient-based steepest ascent search algorithm to find (local) optima in real-time. ESC-based region-2 control for tuning the torque gain, blade pitch angle, and yaw angle was investigated by Creaby et al. [3]. They used rotor power as the feedback. Xiao et al. [4] provided field test results in region-2 using the NREL CART3 turbine. Despite the encouraging outcomes of these ESC investigations, one disadvantage of these techniques is inconsistent convergence rates to the optimal control settings as wind speed changes within region-2. Rotea [5] analyzed the root cause of inconsistent convergence; he proposed a “log-power feedback strategy” for ESC-based wind turbine control. The improved and consistent convergence of the log-power ESC was demonstrated in [5] using a simplified reduced-order model. Afterwards, it was shown through high-accuracy large-eddy simulations that the log-power feedback ESC calibrated at a given wind speed exhibits consistent and robust performance across all wind speeds within region-2 under realistic turbulent wind conditions [6].

Guay et al. [7] recently proposed an ESC algorithm that estimates the gradient using a variant of the recursive least-squares algorithm for parameter estimation. The technique in [7] introduces a proportional-integral approach to improve the transient performance of the extremum-seeking controller. The algorithm in [7] shall be referred to as PIESC. This algorithm is faster than the conventional ESC algorithm.

In this paper, we propose a log-of-power feedback PIESC scheme for region-2 power maximization. The algorithm adjust the torque gain parameter k_g in the “classical $\tau_g = k_g \omega_g^2$ ” (τ_g is the reference generator torque, ω_g is a filtered version of the measured generator speed) control law [1] and the blade pitch angle β for region-2 power maximization individually. Simulation results demonstrate that the combination of the log-of-power transformation with the PIESC scheme yields a fast algorithm for optimal tuning of the torque gain with a less invasive dither signal than currently possible with the conventional log-of-power ESC. We also show results for the optimal tuning of the blade pitch angle with the log-of-power PIESC scheme. Such tuning is useful when changes in blade aerodynamics or the environment result in a different optimal blade pitch angle than the one provided by the manufacturer.

This paper is an extension of the work in [8], which contained initial comparative results for the LP-PIESC and LP-ESC (i.e., a conventional ESC driven by the log-of-power signal) for torque-gain k_g tuning only. Here, we extend these initial results to provide a detailed analysis of energy capture and loads when the LP-ESC and LP-PIESC are used to determine the optimal torque gain. This detailed comparative study demonstrates the faster convergence of the LP-PIESC over the LP-ESC. In addition to faster convergence, we show that the LP-PIESC requires a smaller dither amplitude than the LP-PIESC. We also introduce the use of the LP-PIESC to determine the optimal blade pitch angle in below-rated wind conditions and demonstrate its rapid convergence to the optimal angle.

All simulations are done using the NREL 5-MW reference turbine [2] for a range of wind speeds and turbulence intensities. In order to focus on the evaluations in below-rated wind speeds, we do not implement the baseline NREL 5-MW region switching strategy; instead, we allow the turbine to operate in region-2 for the wind speeds considered. The torque control always follows the $\tau_g = k_g \omega_g^2$ control law for all wind speeds and turbulence intensities.

The organization of the paper is as follows. Background information for the PIESC algorithm and log-of-power feedback is given in Section 2. Section 3 describes the implementation, design parameters, and simulation results of the LP-ESC and LP-PIESC for torque gain control. The LP-PIESC implementation, design parameters, and simulation

results for the case of blade pitch angle control are shown in Section 4. Final remarks are given in Section 5.

2. Background

2.1. Log-Power Maximization Using Gradient-Based Algorithms

Extremum Seeking Control (ESC) and PIEESC are gradient-based algorithms that tune parameters in real-time in order to maximize a system's performance index. These algorithms do not require comprehensive physical models to work. The gradient of the performance index with respect to the parameters is estimated by perturbing the tunable parameters with a zero-mean periodic dither signal. By demodulating a measurement of the perturbed performance index (ESC) or by using variants of recursive least squares (PIEESC), a gradient estimate can be obtained. Then, the values of the tunable parameters are updated according to the estimated gradient. The optimum is reached asymptotically, starting from a suboptimal guess of the parameter values.

Rotea [5] conducted a study for power maximization with gradient-based algorithms that demonstrates the advantages of using the logarithm of the power signal rather than the power itself as the performance index. The intuition behind the result in [5] is relatively simple to explain, and it is summarized as follows.

The power available in the wind is given by

$$P_{\text{wind}} = \frac{1}{2} \pi R^2 \rho V^3 \quad (1)$$

where R is rotor radius in m, ρ is air density in kg/m³, and V is the incoming wind speed perpendicular to the rotor plane in m/s. The rotor power produced can then be given by

$$P = P_{\text{wind}} C_p(u) \quad (2)$$

where C_p denotes the non-dimensional power coefficient of the wind turbine, and u is a control parameter to adjust the power coefficient. In practice, u can be the torque gain of the generator torque control signal, the blade pitch angle, or some other controllable parameter influencing $C_p(u)$.

The goal is to maximize C_p by proper selection of an optimal u -value using measurements of the power P only. When the rotor power is the performance index, the gradient of the performance index (rotor power) with respect to u is

$$\frac{\partial P}{\partial u} = P_{\text{wind}} \frac{\partial C_p(u)}{\partial u} \quad (3)$$

which is proportional to the power available in the wind P_{wind} . However, when the logarithm of the power signal is utilized as the performance index, i.e., $J = \ln P$, the gradient becomes

$$\frac{\partial J}{\partial u} = \frac{\partial}{\partial u} \ln(P_{\text{wind}} C_p(u)) = \frac{1}{C_p(u)} \frac{\partial C_p(u)}{\partial u} \quad (4)$$

which does not depend on the available wind power P_{wind} , and it is only a function of the power coefficient. This result, however simple, has remarkable implications.

Note from (1) and (3) that the convergence properties of gradient-based algorithms using a direct power measurement is a function of V^3 . Thus, without re-tuning, such algorithms will exhibit slow convergence at low wind speeds and may become unstable at high wind speeds [5,6]. On the other hand, if a gradient-based algorithm is used to maximize the log-power performance index, then it follows from (4) that convergence and stability are independent of the wind speed V . This results in an easier-to-tune optimization algorithm which performs consistently throughout region-2. This idea from in [5] is patent-pending [9]. The consistency and robustness of ESC with the log-power performance index are demonstrated in [6] using detailed large-eddy simulations.

2.2. LP-ESC and LP-PIESC

In this paper, we use conventional extremum seeking control (ESC) in continuous time with the logarithm of the rotor power as the performance index to be maximized following the design methodology in [4]. We shall refer to this algorithm as the **LP-ESC**. A typical LP-ESC is shown in Figure 1, where $F_{in}(s)$ and $F_{out}(s)$ are unity-gain linear time-invariant (LTI) approximation of the input and output dynamics, respectively, and $f(u)$ represents a static map of the performance index (rotor power). A periodic dither signal $d_1(t) = a \sin(\omega t)$ and a demodulation signal $d_2(t) = \sin(\omega t + \theta)$ are applied to estimate the gradient $\partial f / \partial u$, where a is the dither amplitude, ω is the dither frequency, and θ represents the phase compensation angle. The high-pass filter $F_{HP}(s)$ is applied to the logarithm of the performance index $\ln(y)$ to eliminate the steady-state term of the objective function. Following the multiplication by $d_2(t)$, a low-pass filter $F_{LP}(s)$ extracts the gradient information. The LP-ESC loop is closed by an integrator with gain k to drive $\partial f / \partial u$ to zero asymptotically.

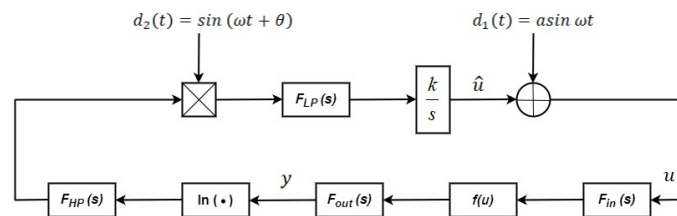


Figure 1. LP-ESC: Conventional ESC with log power feedback.

Our goal is to develop an improved version of the LP-ESC using the proportional plus integral ESC (PIESC) developed by Guay et al. [7]. We shall refer to this gradient-based algorithm as the **LP-PIESC**.

The LP-PIESC holds the promise of faster convergence than the LP-ESC due to two main modifications: the use of a recursive least squares-like method to estimate the gradient and the addition of a proportional term to accelerate convergence to the optimum. In the proposed proportional-integral extremum seeking control, the gradient estimation is done using parameter estimation instead of the conventional dither-demodulation technique. The development of the LP-PIESC is based on a time-varying estimate of the gradient of the cost and a PI control law to drive the system to its optimal operating point.

The proportional-integral extremum seeking controller proposed in [7] is given by (5) and can be represented as in Figure 2:

$$\begin{cases} u = -k_p \hat{\theta}_1 + \hat{u} + d_1(t) \\ \dot{\hat{u}} = -\frac{1}{\tau_I} \hat{\theta}_1 \end{cases} \quad (5)$$

where k_p is the proportional gain, τ_I is the time constant, and $\hat{\theta}_1$ is proportional to the gradient $\partial f / \partial u$.

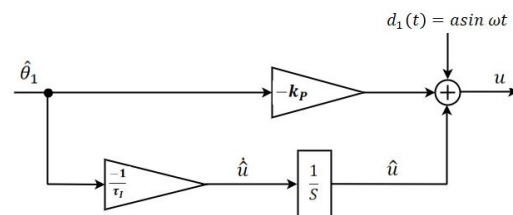


Figure 2. PI controller used for LP-PIESC.

The parameter to be estimated as presented in [7] is $\theta = [\theta_0, \theta_1]^T$, where the superscript T denotes transpose. In our application, θ is a real-valued vector of dimension two. Only the scalar component θ_1 contains the gradient information we need. The parameter θ_0 is

a bias component needed for the parameter estimation to work properly. The parameter estimation update law is given by

$$\dot{\hat{\theta}} = \text{Proj}(\Sigma^{-1}(c(e - \hat{\eta}) - \sigma\hat{\theta}), \hat{\theta}) \quad (6)$$

where $\text{Proj}(\cdot)$ is a Lipschitz projection operator designed to ensure that the estimates are bounded within the constraint set and guarantee stability. This projection algorithm was implemented as discussed in Appendix E in [10] and the constraint set adaptation was adopted as per Adetola et al. [11]. The forcing term in the differential Equation (6) is the prediction error e given by

$$e = y - \hat{y} \quad (7)$$

where y is the logarithm of the performance index to be optimized and \hat{y} represents its prediction. The equation for the predicted output \hat{y} is given by the following dynamics:

$$\dot{\hat{y}} = \phi^T \hat{\theta} + K e + c^T \hat{\theta} \quad (8)$$

where $\phi = [1, (u - \hat{u})]^T$ and K is a positive constant to be determined.

The time-varying parameter c in (8) is the solution of the differential equation

$$\dot{c}^T = -K c^T + \phi^T \quad (9)$$

An auxiliary variable η is introduced and its filtered estimate is given by

$$\dot{\hat{\eta}} = -K \hat{\eta} \quad (10)$$

The matrix Σ is the solution of the matrix differential equation

$$\dot{\Sigma} = c c^T - k_T \Sigma + \sigma I \quad (11)$$

with $\Sigma(0) = \alpha I$ and $\alpha > 0, \sigma > 0, k_T > 0$, i.e., they are positive constants. The inverse of Σ is given by the solution of the matrix differential equation

$$\dot{\Sigma}^{-1} = -\Sigma^{-1} c c^T \Sigma^{-1} + k_T \Sigma^{-1} - \sigma \Sigma^{-2} \quad (12)$$

with $\Sigma^{-1}(0) = \frac{1}{\alpha} I$. The estimation algorithm propagates Σ^{-1} , which is used in the parameter dynamics (6).

3. Implementation of LP-ESC and LP-PIESC for Torque Control in Region-2

The 5MW NREL reference turbine model, simulated with OpenFAST, is used in this study [12]. Table 1 lists the major parameters of this turbine model.

Table 1. Main parameters of NREL 5MW turbine used for algorithm designs.

Description	Value
Rating	5 MW
Rotor radius (R)	63 m
Gear Ratio (N)	97
Rotor Inertia (I_r)	35,444,067 kg·m ²

The generator torque (τ_g) is generally used as the control variable to maximize power in region-2 and is computed as a tabulated function of the filtered generator speed in NREL's baseline control strategy. The main control law to maximize power below-rated wind speeds is given by

$$\tau_g = k_g \omega_g^2 \quad (13)$$

where ω_g denotes the generator speed and k_g is the generator torque gain used as the control parameter for the extremum seeking algorithms. The theoretical optimal value of k_g is obtained from [1]

$$k_{\text{opt}} = \frac{1}{2} \frac{\rho A R^3 C_{p,\text{max}}}{N^3 \lambda_{\text{opt}}^3} \quad (14)$$

where A is the cross-sectional area swept by the rotor and ρ is the air density given by 1.22 kg/m^3 . For this turbine, the theoretical optimal tip-speed ratio is $\lambda_{\text{opt}} = 7.55$ and the corresponding maximum power coefficient is $C_{p,\text{max}} = 0.48$ [2]. Then, the optimal generator torque gain takes the value $k_{\text{opt}} = 2.34 \text{ Nm}/(\text{rad/s})^2$.

The control parameter u is the non-dimensional normalized torque gain introduced in [5]. The optimal normalized torque gain value is

$$u_{\text{opt}} = \frac{k_{\text{opt}}}{I_r} \times N^3 \approx 0.061 \quad (15)$$

A high-level block diagram of the region-2 torque gain LP-ESC/LP-PIESC implementation is depicted in Figure 3. Input to the LP-ESC/LP-PIESC is the logarithm of the rotor power P normalized with respect to the rated power $P_r = 5 \text{ MW}$. A rate limit of 15 kNm/s is applied on the torque reference as per the definition of the 5-MW turbine to avoid sudden change in the torque command [2].

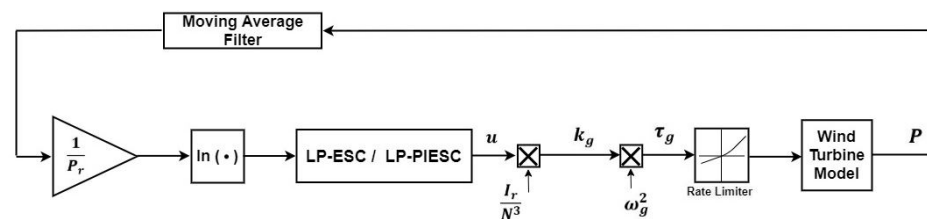


Figure 3. LP-ESC/LP-PIESC implementation.

3.1. Parameter Design

LP-ESC parameters are designed following the guidelines in [13,14]. The dither frequency is chosen within the bandwidth of the plant dynamics. The rotor inertia and the actuator dynamics yield the input dynamics, while the output dynamics is due to the sensor dynamics and/or signal conditioning. The input and output dynamics are merged at the plant input and approximated using open-loop step responses under constant wind input to simplify the algorithm design. The response of the rotor speed (ω_r) under staircase step changes in normalized torque-gain indicates a first-order dynamics, as shown in Figure 4. The test was performed for the hub-height mean wind speed of 8 m/s with no turbulence. The estimated time constant from the normalized torque-gain to the rotor speed ranges from 7 to 8 s . The largest time constant was adopted for ESC design, i.e., 8 s . The corresponding bandwidth of the combined input–output dynamic for the torque-gain ESC is 0.125 rad/s . As dither frequency should be selected within the estimated bandwidth, it was selected as 0.02 rad/s . Figure 5 shows the Bode plots for the estimated plant dynamic and the filters in the ESC design. The low-pass F_{LP} and high-pass F_{HP} filters (see Figure 1) are first-order filters. The dither amplitude was selected using trial and error. The dither amplitude is about 33% of the optimal normalized torque gain in (15). The integrator gain k was designed to achieve a settling time $T_s = 15 \text{ min}$, approximately for the 8 m/s wind speed with 10% TI case and then the same integrator gain was used for all other cases. The settling time T_s is defined as the time it takes to reach optimum torque gain value for the first time after turning on the dithering (control on). The LP-ESC parameters used are listed in Table 2.

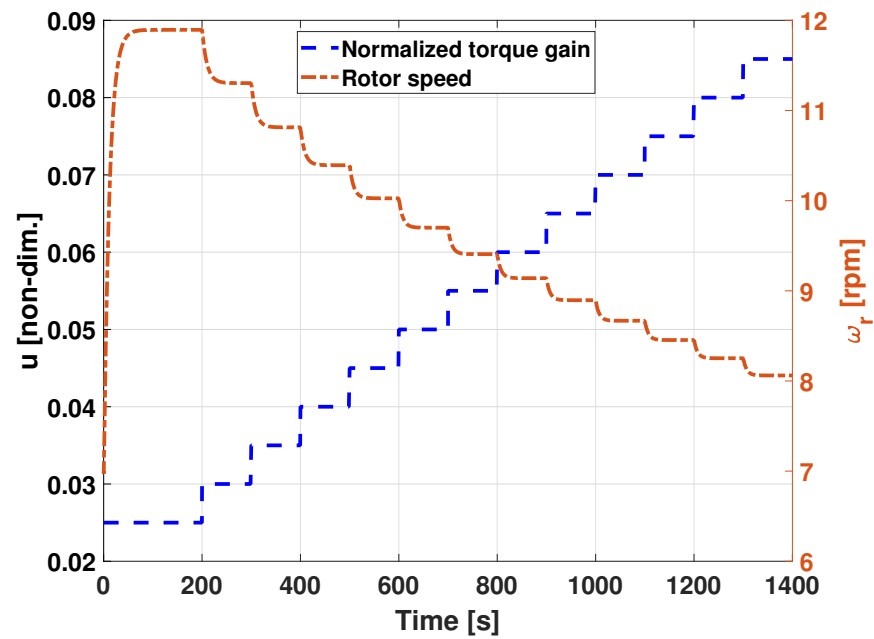


Figure 4. Rotor speed dynamics for step changes in u ($V = 8$ m/s).

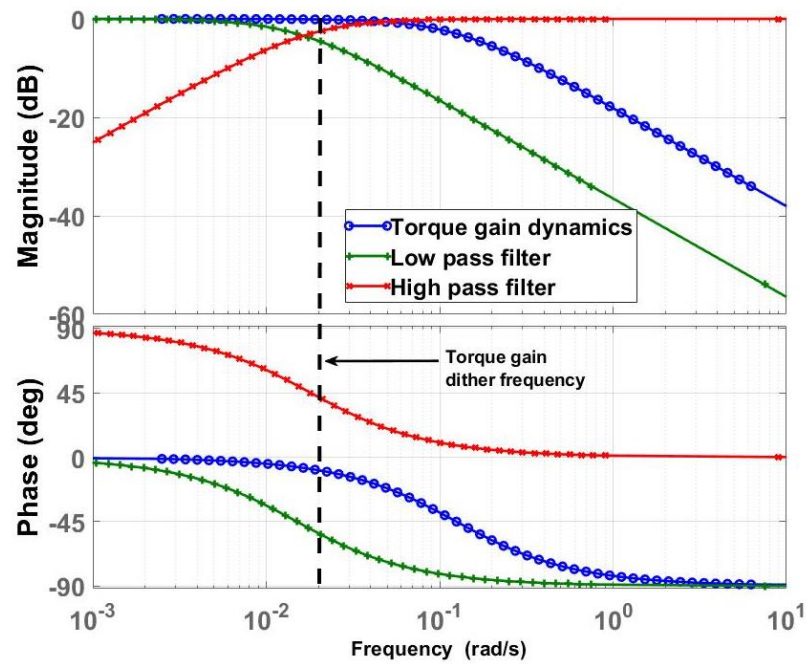


Figure 5. Bode Plot of input dynamics, LPF, HPF, and the dither frequency.

Table 2. LP-ESC Parameters of NREL 5MW Region 2 controller (see Figure 1).

Parameter	Torque-Gain LP-ESC
Dither Frequency (ω)	0.02 rad/s
Dither Amplitude (a)	0.02 (non-dimensional)
Cut-off Frequency of LPF	0.015 rad/s
Cut-off Frequency of HPF	0.018 rad/s
Phase Compensation (θ)	0.36 rad
Integrator Gain (k)	0.001 rad/s

The LP-PIESC scheme was designed to have the same dither frequency as the LP-ESC. After trial and error, the dither amplitude could be reduced significantly to 25% of the dither amplitude value of LP-ESC. This result is important because the external dither is a perturbation to the overall turbine. One plausible explanation for the smaller dither amplitude is that the method for gradient estimation in LP-PIESC, Equations (6)–(12), is more sophisticated than the one used in the conventional LP-ESC. The parameters for the LP-PIESC scheme are listed in Table 3.

Table 3. LP-PIESC Parameters of NREL 5 MW Region 2 controller. See Equations (6)–(12).

Parameter	Torque-Gain LP-PIESC
Dither Frequency (ω)	0.02 rad/s
Dither Amplitude (a)	0.005 (non-dimensional)
k_T	20 rad/s
K	20 rad/s
σ	10^{-6} (s/rad) ²
k_p	0.000005 s/rad
τ_I	2.8 (non-dimensional)

3.2. Simulation Results

The LP-ESC and the LP-PIESC controllers with the algorithm parameters shown in Tables 2 and 3 are evaluated with OpenFAST simulations for different hub-height mean wind speeds of 4 m/s, 8 m/s, and 12 m/s, no wind shear, and under turbulence intensities (TI) of 10% and 15%, respectively.

The turbulent wind profiles were generated using NREL TurbSim [15]. TurbSim uses IEC 61400-1 [16] to generate the wind profiles. In order to generate the wind input files for our simulations, we specify the following five parameters in the meteorological boundary conditions section of the TurbSim input file (defined in Appendix A of [15]): (1) Turbulence model is set as Kaimal (IECKAI), (2) IEC turbulence type is chosen to be the Normal Turbulence Model (NTM), (3) hub-height of 90 m for NREL 5MW reference turbine model, (4) mean wind speed, and (5) percentage turbulence intensity. Other parameters were left to their default values in TurbSim. Mathematical expression for the Kaimal spectrum can be found in Appendix C.3 of [17].

Figure 6 shows the hub-height wind time series for the three mean wind speeds (i.e., 4 m/s, 8 m/s, and 12 m/s) used in the simulation study with 10% TI. These wind profiles are then used to evaluate the performance of LP-ESC and LP-PIESC in Figures 7 and 8, respectively. The top plot shows the normalized torque gain (u), the middle plot shows the tip speed ratio (λ), and the estimated power coefficient (C_p) is shown in the bottom plot. Tip speed ratio (λ) and the estimated power coefficient (C_p) plots are obtained by applying a 100 s moving average filter on the OpenFAST outputs for these variables. The vertical dashed lines in Figure 7 show the time LP-ESC is turned on and the time for practical convergence to the optimum power coefficient C_p . Both LP-ESC and LP-PIESC are turned on at 150 s.

It can be observed that the LP-ESC takes approximately 850 s (i.e., ≈ 15 min as designed) to converge to the optimum torque gain for 8 m/s and 12 m/s mean wind speeds. In stark contrast, the LP-PIESC converges to the optimum almost instantaneously for all cases.

Simulations with increased turbulence intensity (15% TI) are also used to evaluate the performance of LP-PIESC. The simulation results are shown in Figure 9. It can be observed that increasing the turbulent intensity does not affect the transient or steady-state performance of the LP-PIESC.

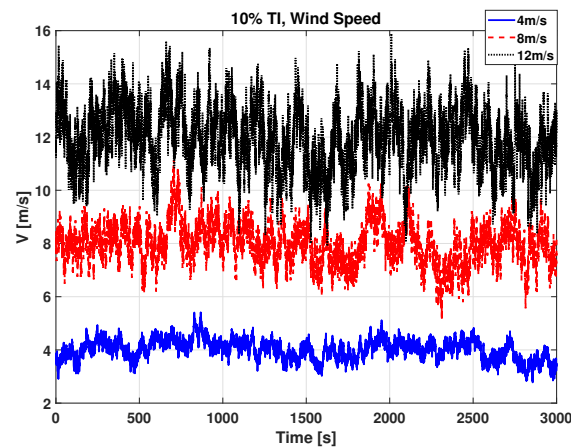


Figure 6. Wind speed time series at hub height: mean wind speeds 4 m/s, 8 m/s, 12 m/s and 10% turbulence intensity.

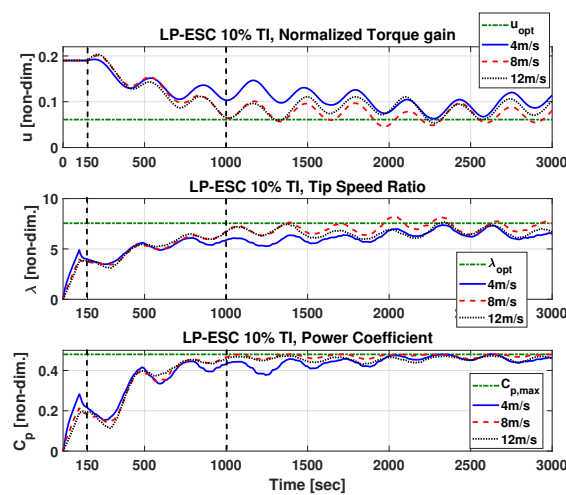


Figure 7. Performance of LP-ESC with the parameters shown in Table 2 and hub-height wind from Figure 6. Normalized torque gain u (top), tip speed ratio λ (middle), estimated power coefficient C_p (bottom). The dashed horizontal lines indicate optimal parameters u_{opt} , λ_{opt} and $C_{p,max}$. Vertical dashed lines in u show the point LP-ESC is turned on (150 s) and the point where it reaches practical convergence.

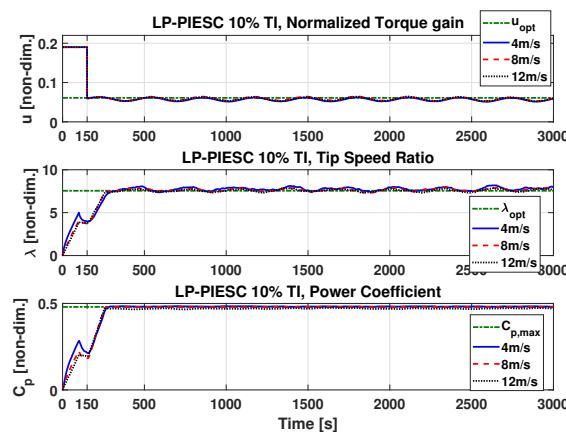


Figure 8. Performance of LP-PIESC with the parameters shown in Table 3 and hub-height wind from Figure 6. Normalized torque gain u (top), tip speed ratio λ (middle), estimated power coefficient C_p (bottom). The dashed horizontal lines indicate optimal parameters u_{opt} , λ_{opt} and $C_{p,max}$. The LP-PIESC is turned on at 150 s.

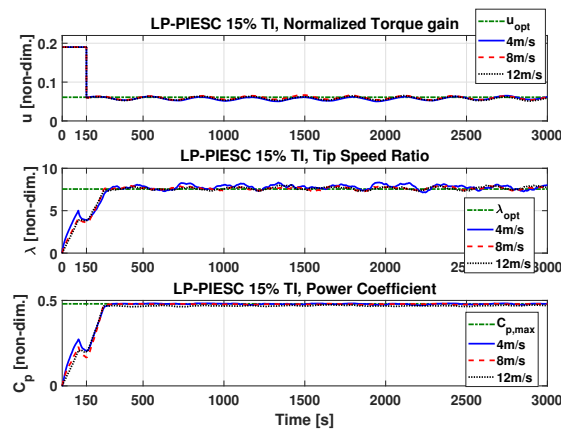


Figure 9. Performance of LP-PIESC with the parameters shown in Table 3 and wind input with 15% TI. Normalized torque gain u (top), tip speed ratio λ (middle), and estimated power coefficient C_p (bottom). The dashed horizontal lines indicate optimal parameters u_{opt} , λ_{opt} and $C_{p,max}$. The LP-PIESC is turned on at 150 s.

The results in this section provide evidence that LP-PIESC is faster to converge to the optimum than LP-ESC and also robust to the variations in mean wind speed and turbulence intensities. In addition, the LP-PIESC requires a dither amplitude significantly lower than that for LP-ESC.

3.3. Energy Capture

The energy capture for both the LP-ESC and the LP-PIESC controllers is evaluated and compared with the baseline controller (i.e., optimal torque gain value at all times). The controllers are evaluated for the hub-height mean wind speeds of 4 m/s, 8 m/s, and 12 m/s, no wind shear and turbulence intensities (TI) of 10% and 15%, respectively. TurbSim [15] is used to generate wind profiles from six distinct seeds for each turbulent intensity case. The average energy capture over those six wind profiles will be presented here. All the calculations are done using data from the time the extremum seeking controllers are turned on (150 s) till the end of the simulation (3000 s).

First, the LP-ESC is compared with the baseline controller. The result for average energy output can be seen in Figure 10. Using LP-ESC results in an average energy loss of approximately 13% (TI = 10%) and 16% (TI = 15%), respectively.

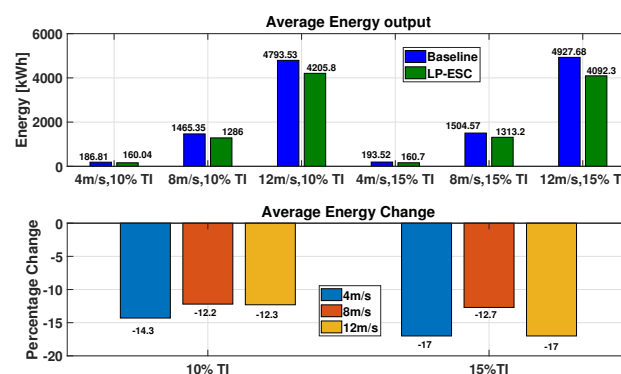


Figure 10. Energy capture comparison: Baseline vs. LP-ESC. Average energy output with baseline optimal torque gain and LP-ESC (top), percentage change in energy capture (bottom).

The energy capture with LP-PIESC was also compared with the baseline controller. The average change in energy capture is shown in Figure 11.

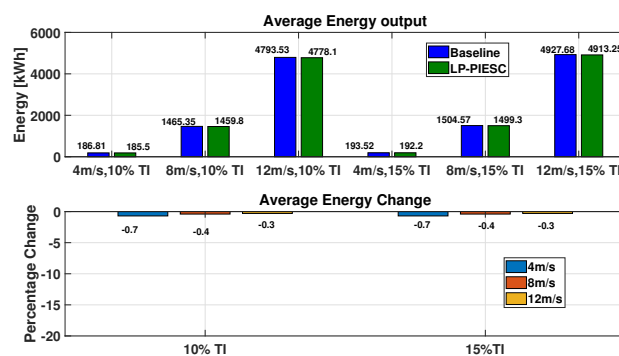


Figure 11. Energy capture comparison: Baseline vs. LP-PIESC. Average energy output with baseline optimal torque gain and LP-PIESC (top), percentage change in energy capture (bottom).

The results suggest that the LP-PIESC gives an energy output very close to the baseline controller, where the optimal tuning parameter (torque gain for our study) value is known. The maximum energy loss was 0.7% (reduction of around 1 kWh) which was seen for the low wind speed of 4 m/s. Averaging results across all wind conditions for both LP-ESC and the LP-PIESC, we obtain Table 4.

Table 4. Average energy capture for both LP-ESC and LP-PIESC compared to baseline.

	Baseline (kWh)	LP-ESC (kWh)	% Change
Average Energy Output	2178.6	1869.7	−14.2
	Baseline (kWh)	LP-PIESC (kWh)	% Change
Average Energy Output	2178.6	2171.4	−0.3

Table 4 suggests that due to the faster convergence of the torque gain to its optimal value, the LP-PIESC could produce nearly optimal energy output. That is, the LP-PIESC could reach very close to the maximum energy output without knowing the optimal setting. This optimal setting in the baseline controller could change over time due to the wear and tear of blade surfaces and variations in atmospheric and environmental conditions such as icing, insects, etc. In this case, the baseline controller can result in a loss of energy. The LP-PIESC could aid in finding the new optimal torque gain value without any significant loss in energy capture.

3.4. Structural Loads Analysis

This section shows the change in loads (tower, drive train, blades) due to the change in torque gain imparted by the LP-PIESC. We investigate the impact on transient loads caused by the sudden change in torque gain as well as the impact of the dither signal on the wind turbine loads. The loads considered are shown in Table 5, along with the natural frequencies of the relevant structural modes obtained from [2,18].

Table 5. Blade, drivetrain, and tower loads considered for analysis with respective natural frequencies.

Load	First Mode Natural Frequency (Hz)
Blade-root flapwise bending moment (BRFW)	0.5–1
Blade-root edgewise bending moment (BREW))	0.9–1.3
Drivetrain torsional moment (DTT)	1.7
Tower-base fore-aft bending moment (TBFA)	0.32
Tower-base side-side bending moment (TBSS)	0.31

The controllers are evaluated for the hub-height mean wind speeds of 4 m/s, 8 m/s, and 12 m/s, no wind shear and turbulence intensities (TI) of 10% and 15%, respectively.

TurbSim [15] is used to generate wind profiles from six distinct seeds for each turbulent intensity case. The time series of the loads are analyzed with MLife to calculate aggregate damage equivalent loads (DELs) [19]. The DELs obtained from the time series of the LP-PIESC are then compared against those obtained from the baseline controller. All the evaluations are done on the data from 150 s till the simulation end time, i.e., 3000 s.

As shown in Figures 8 and 9, when the LP-PIESC is turned on, there is a sudden change in torque gain from the initial setting to the optimal value. This sudden change will propagate to a step-change in the generator torque because the rotor speed cannot change instantaneously. Figure 12 illustrates this situation for the wind speeds shown in Figure 6. The response of the baseline constant torque gain is shown as well. As expected, the generator torque and the rotor angular speed converges to the optimal time series, eventually.

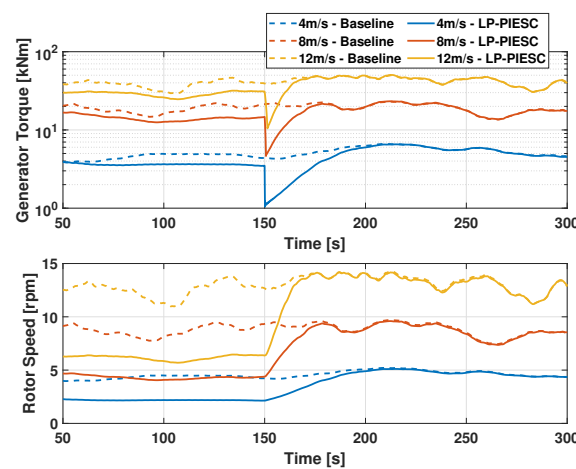


Figure 12. Effect of sudden change in torque gain with LP-PIESC on generator torque (top) and rotor speed (bottom) compared with the baseline (for hub height wind from Figure 6).

3.4.1. Drivetrain Loads

The first turbine component affected by sudden changes in generator torque is expected to be the drivetrain. DEL result obtained from the time series data of drivetrain torsion (DTT) from ESC start, i.e., 150 s to simulation end time, i.e., 3000 s is as shown in Figure 13.

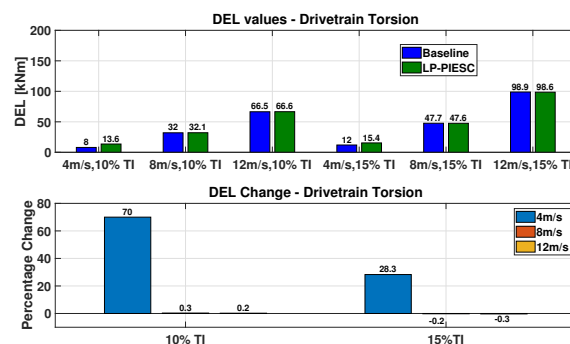


Figure 13. Drivetrain torsion comparison: Baseline vs. LP-PIESC. Aggregate DEL values with baseline controller and LP-PIESC (top), percentage change in DEL (bottom) for time series from 150 s to 3000 s.

DTT does not show much change for 8 m/s and 12 m/s wind speeds at 10% and 15% TI but increases for 4 m/s wind speed by 70% at 10% TI and 28% at 15% TI, respectively. The high percentage change is largely due to the smaller values at a low wind speed of

4 m/s. The actual difference in DEL values is 5.6 kNm for 10% TI and 3.4 kNm for 15% TI wind.

To better understand the large percentage change in the DTT DEL at 4 m/s, we examine the time series for the wind profile in Figure 6, which corresponds to one of the input wind files used to calculate damage equivalent loads. Figure 14 shows the time series of the drivetrain torsional moment. Note the large increase in the amplitude of the drivetrain torsion signal at 150 s (LP-PIESC turned on).

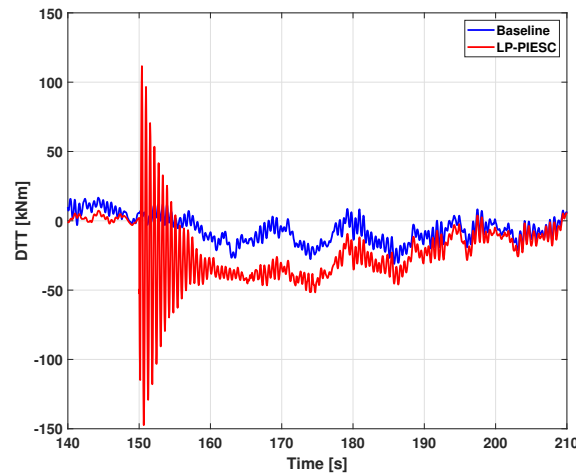


Figure 14. Drivetrain Torsion (DTT) time series of baseline (blue) and LP-PIESC (red) for the 4 m/s wind profile in Figure 6. Sudden change in generator torque at LP-PIESC start, i.e., 150 s leads to an increase in the amplitude of the drivetrain torsional moment. Once the transients die out, it follows the baseline.

These larger oscillations have a frequency of approximately 1.7 Hz, which corresponds to the drivetrain natural frequency shown in Table 5. This result suggests that the percentage change in DELs at low wind speed, when the dimensional moments are small, can be attributed to the natural transient response of the drive train to a sudden change in one of its inputs, i.e., the generator torque. To increase confidence in this explanation, the DELs are also computed using the time series from 300 s to the end of the simulation (3000 s). The results are shown in Figure 15. It can be observed that once the transients die out (Figure 14) due to the sudden change in torque (Figure 12), the DELs obtained from the LP-PIESC are almost identical to that of the baseline controller, which supports our hypothesis.

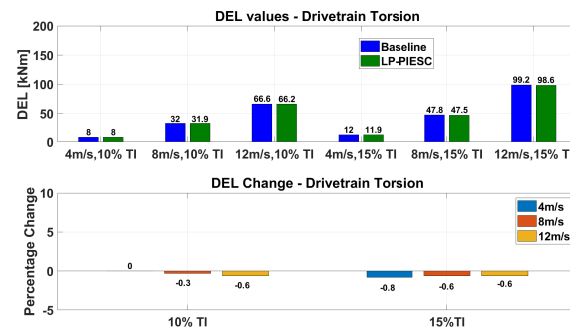


Figure 15. Drivetrain torsion comparison: Baseline vs. LP-PIESC. Aggregate DEL values with baseline controller and LP-PIESC (top), and percentage change in DEL (bottom) for time series from 300 s to 3000 s.

In addition, from Figure 15 we note the continuous presence of the dither signal does not affect the drive train DELs, that is, the DELs with the LP-PIESC are almost identical to the ones with the constant torque gain.

3.4.2. Tower Loads

Next, we studied the two fundamental mechanical moments that must be considered, one is related to the forward and backwards motion of the tower (tower-base fore-aft bending moment (TBFA)) and the other is related to the side-side tower motion (tower-base side-to-side bending moment (TBSS)). DEL results for the tower loads are shown in Figures 16 and 17.

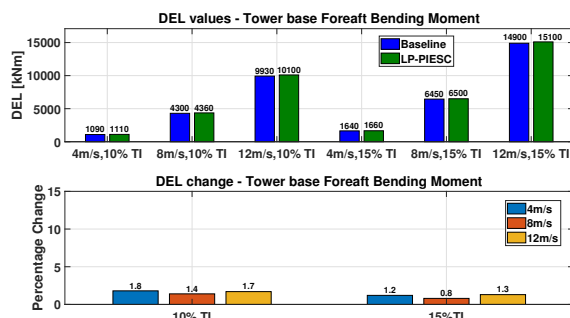


Figure 16. Tower- base fore-aft bending moment comparison: Baseline vs. LP-PIESC. Aggregate DEL values with baseline controller and LP-PIESC (top), percentage change in DEL for time series from 150 s to 3000 s.

The average change in DEL of TBFA across all wind speeds is between 1.1% (15% TI) and 1.6% (10% TI). The actual DEL values obtained with the LP-PIESC are very close to the baseline DEL values, which means that the effect of the sudden change in generator torque and that of the dither signal with the LP-PIESC do not affect the TBFA.

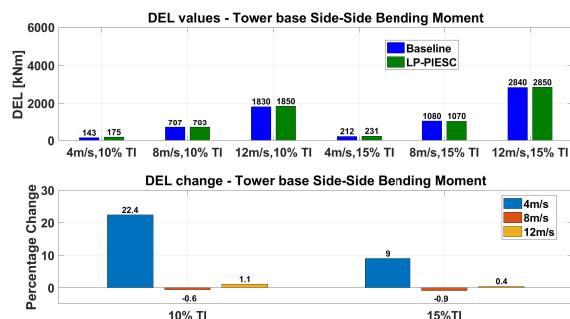


Figure 17. Tower-base side-side bending moment comparison: Baseline vs. LP-PIESC. Aggregate DEL values with baseline controller and LP-PIESC (top), percentage change in DEL (bottom) for time series from 150 s to 3000 s.

For TBSS (Figure 17), there is no substantial change in DEL values at 8 m/s and 12 m/s. On the other hand, at 4 m/s DEL values increase 22% for TI = 10% and 9% for TI = 15%. Again, this percentage value is higher because of the smaller numbers at 4 m/s wind speed. That is, the actual difference in DEL values is 32 kNm (10% TI) and 19 kNm (15% TI). The TBSS experiences two effects: (i) as the LP-PIESC starts with a highly sub-optimal initial torque gain value, the initial transient is high, and it takes more than 150 s to converge, and (ii) the effect of switching on the LP-PIESC at 150 s. Therefore, examining the TBSS DEL after these two effects have died out would be meaningful as it is difficult to separate their effects. Therefore, we also evaluated the TBSS DELs using the time series from 300 s to the end of the simulation (3000 s). The results are shown in Figure 18. We can observe that the DEL values for both the LP-PIESC and the baseline are almost identical. The continuous presence of the dither signal in the LP-PIESC does not affect the TBSS DELs.

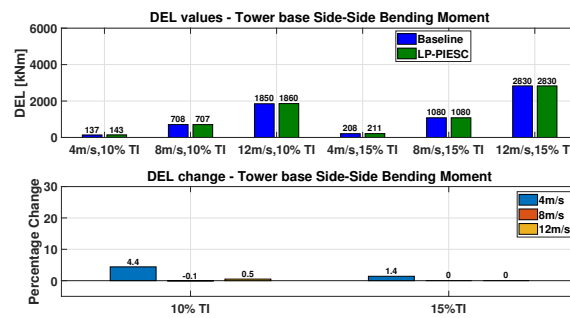


Figure 18. Tower-base side-side bending moment comparison: Baseline vs. LP-PIESC. Aggregate DEL values with baseline controller and LP-PIESC (top), percentage change in DEL (bottom) for time series from 300 s to 3000 s.

3.4.3. Blade Loads

For blade loads, blade root edgewise bending moment (BREW) and blade-root flapwise bending moment (BRFW) were selected for analysis. DEL results for the blade loads are shown in Figures 19 and 20. For each wind condition, the corresponding blade load DEL is the average DEL over all three blades.

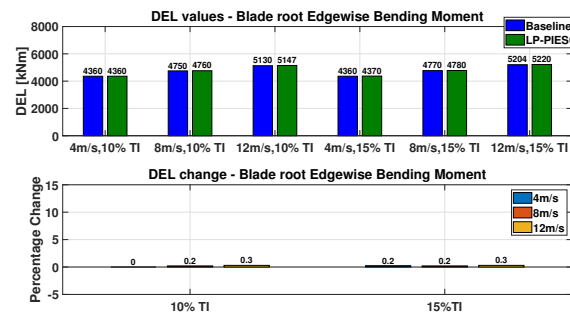


Figure 19. Blade-root edge-wise bending moment comparison: Baseline vs. LP-PIESC. Aggregate DEL values with baseline controller and LP-PIESC (top), percentage change in DEL (bottom) for time series from 150 s to 3000 s.

The average change in DEL of BREW across all wind speeds is between 0.2% (10% TI) and 0.3% (15% TI). The actual DEL values obtained with the LP-PIESC are very close to the baseline DEL values. It means that the effect of the sudden change in generator torque and that of the dither signal with the LP-PIESC do not affect the BREW.

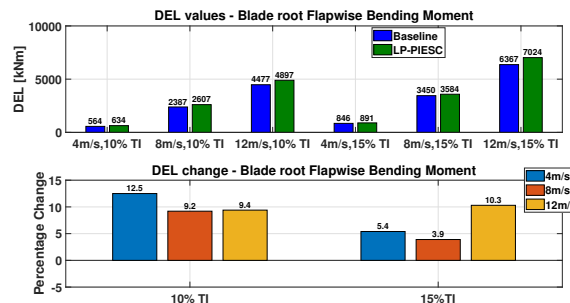


Figure 20. Blade-root flap-wise bending moment comparison: Baseline vs. LP-PIESC. Aggregate DEL values with baseline controller and LP-PIESC (top), percentage change in DEL (bottom) for time series from 150 s to 3000 s.

For BRFW, 4 m/s with 10% TI and 12 m/s with 15% TI show more than 10% increase in DEL. The reason for the increase is similar to the case for the tower base fore-aft moment; thus, we evaluate DELs from 300 s to simulation end (3000 s), and the results are as shown

in Figure 21. The DEL values for both the LP-PIESC and the baseline are almost identical and the presence of the dither signal in the LP-PIESC does not affect the BRFW DELs.

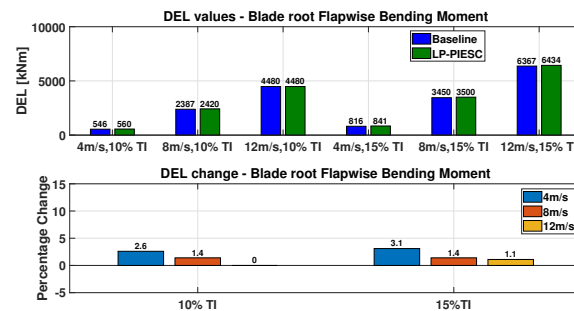


Figure 21. Blade-root flap-wise bending moment comparison: Baseline vs. LP-PIESC. Aggregate DEL values with baseline controller and LP-PIESC (**top**), percentage change in DEL (**bottom**) for time series from 300 s to 3000 s.

4. Implementation of LP-PIESC for Blade Pitch Tuning in Region-2

Given the promising results LP-PIESC showed for the torque gain control in the previous section, in this section, we design and evaluate the LP-PIESC algorithm for the control parameter of blade pitch angle, keeping the normalized torque gain at its optimal value as given in (15). As in the prior section, the design and analysis are done using the NREL 5 MW turbine model in OpenFAST. A high-level block diagram of the blade pitch tuning for region-2 is shown in Figure 22, where u is the blade pitch angle reference commanded by the LP-PIESC. A rate limit of $8^\circ/\text{s}$ is applied on the blade pitch angle reference as per the definition of the 5-MW reference turbine model. The optimal blade pitch angle β for this turbine is 0° .

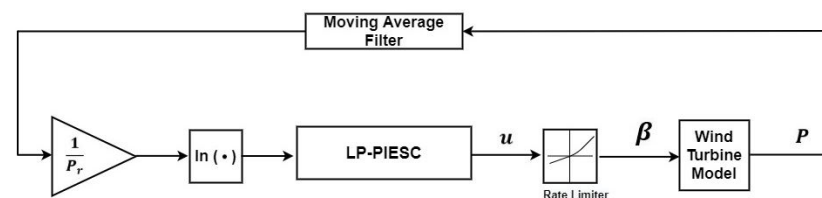


Figure 22. LP-PIESC implementation for blade pitch tuning.

4.1. Parameter Design

As done in Section 3.1, LP-PIESC parameters are designed for blade pitch angle control. The response of the rotor speed under staircase step changes in the blade pitch angle indicates a first-order dynamics, as shown in Figure 23. The test was performed for the hub-height mean wind speed of 8 m/s with no turbulence. The estimated time constant from the blade pitch angle (β) to the rotor speed (ω_r) ranges from 7 to 10 s. The largest time constant was adopted for ESC design, i.e., 10 s. The corresponding bandwidth of the combined input–output dynamic for the blade-pitch ESC is 0.1 rad/s. As the dither frequency should be selected within the estimated bandwidth, it was selected as 0.02 rad/s. The Bode plot for the estimated plant dynamic is shown in Figure 24. The dither amplitude was selected using trial and error. The parameters for the LP-PIESC scheme are listed in Table 6.

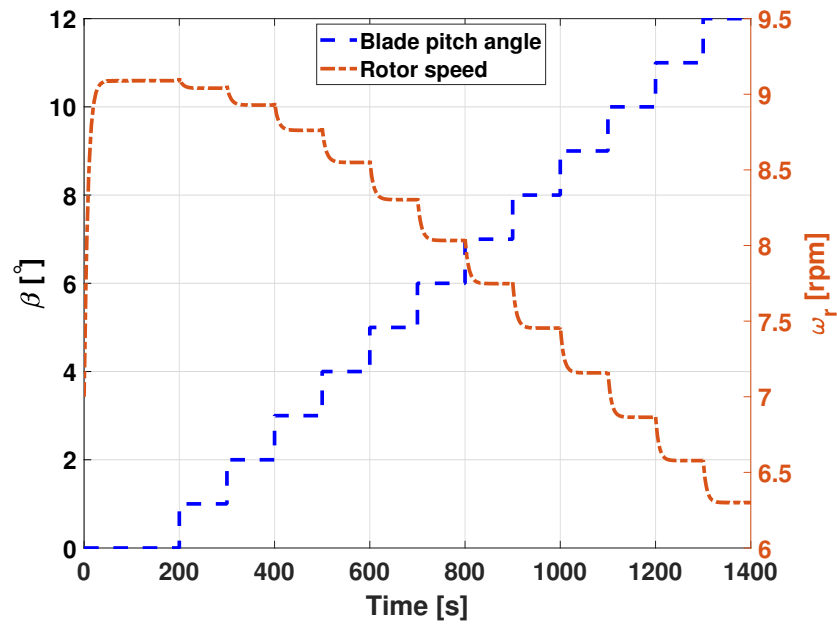


Figure 23. Rotor speed dynamics for step changes in β ($V = 8$ m/s).

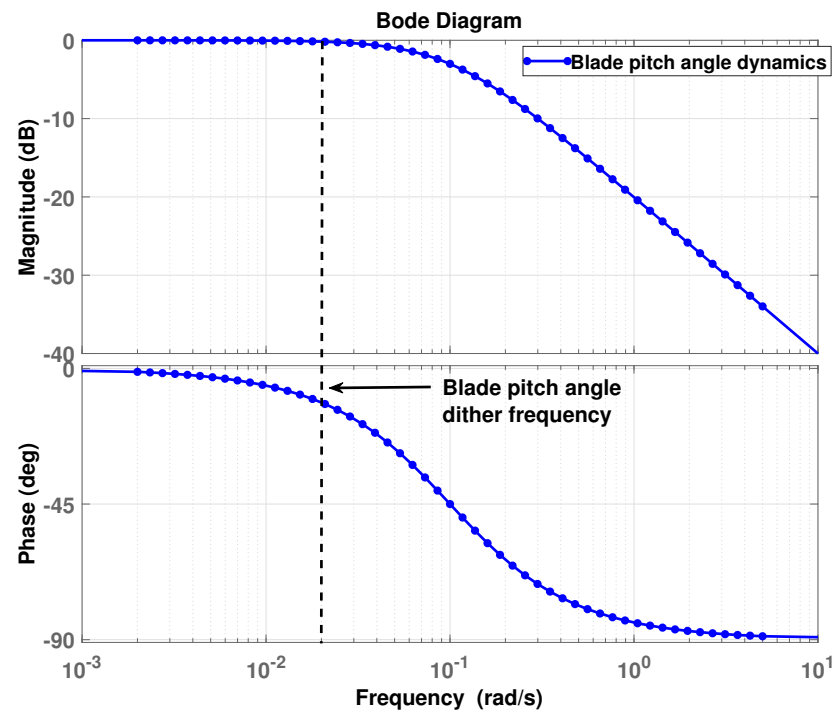


Figure 24. Bode Plot of input dynamics, and the dither frequency.

Table 6. LP-PIESC Parameters of NREL 5 MW Region 2 blade pitch controller. See Equations (6)–(12).

Parameter	Blade-Pitch LP-PIESC
Dither Frequency (ω)	0.02 rad/s
Dither Amplitude (a)	0.2 deg.
k_T	20 rad/s
K	20 rad/s
σ	10^{-6} (deg.s/rad) ²
k_p	0.000005 deg. ² s/rad
τ_I	2.8 deg. ⁻²

4.2. Simulation Results

As done in Section 3.2, the LP-PIESC controller with the parameters shown in Table 6 is evaluated with OpenFAST simulations for different hub-height mean wind speeds of 4 m/s, 8 m/s, and 12 m/s, no wind shear and turbulence intensities (TI) of 10% and 15%, respectively. The wind profiles in Figure 6 with 10% TI are used to determine the performance of the LP-PIESC in Figure 25. The top plot shows the blade pitch angle (β), the middle plot shows the tip speed ratio (λ), and the estimated power coefficient (C_p) is shown in the bottom plot. Tip speed ratio (λ), and the estimated power coefficient (C_p) plots are obtained by applying a 100 s moving average filter on the OpenFAST outputs for these variables. The horizontal dashed lines indicate the optimal values of β , λ , and C_p . The LP-PIESC is turned on at 150 s.

It can be observed that the LP-PIESC converges to the optimum blade pitch angle almost instantaneously for all cases. The tip speed ratio (λ) and the estimated power coefficient (C_p) converges in less than 100 s.

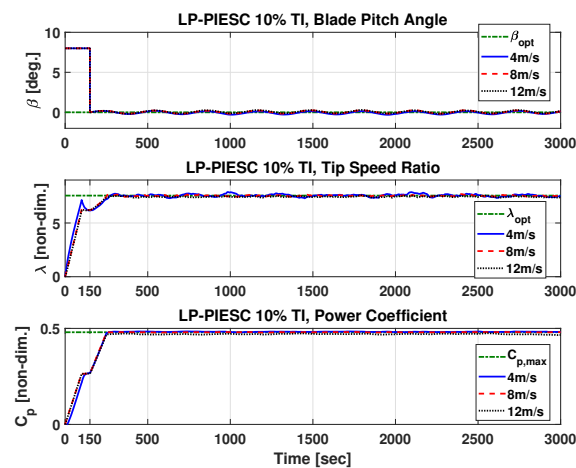


Figure 25. Performance of LP-PIESC with the parameters shown in Table 6 and hub-height wind from Figure 6. Blade pitch angle β (top), tip speed ratio λ (middle), and estimated power coefficient C_p (bottom). The dashed horizontal lines indicate optimal parameters β_{opt} , λ_{opt} and $C_{p,max}$. The LP-PIESC is turned on at 150 s.

Simulations with increased turbulence intensity (15% TI) are also used to evaluate the performance of LP-PIESC. The simulation results are shown in Figure 26. It is observed that increasing the turbulent intensity does not affect the transient or steady-state performance of the LP-PIESC.

The results in this section provide further evidence that LP-PIESC has fast convergence to the optimum and is also robust to the variations in mean wind speed and turbulence intensities.

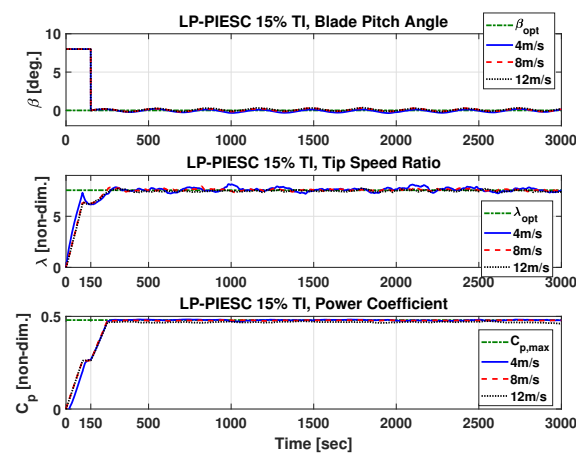


Figure 26. Performance of LP-PIESC with the parameters shown in Table 6 and wind input with 15% TI. Blade pitch angle β (top), tip speed ratio λ (middle), estimated power coefficient C_p (bottom). The dashed horizontal lines indicate optimal parameters β_{opt} , λ_{opt} and $C_{p,max}$. The LP-PIESC is turned on at 150 s.

4.3. Energy Capture

The energy capture for the LP-PIESC controller is evaluated and compared with the baseline controller (i.e., 0° optimal blade pitch angle at all times). The controller is evaluated for hub-height mean wind speeds of 4 m/s, 8 m/s, and 12 m/s, no wind shear and, turbulence intensities (TI) of 10% and 15%, respectively. TurbSim [15] is used to generate wind profiles from six distinct seeds for each turbulent intensity case. The average energy capture is calculated over those six wind profiles. All the calculations are done using data from the time the LP-PIESC is turned on (150 s) till the end of the simulation (3000 s).

The average change in energy capture is shown in Figure 27.

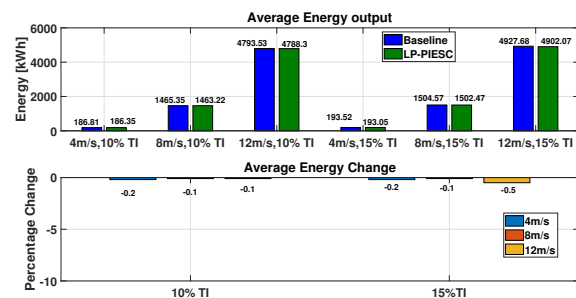


Figure 27. Energy capture comparison: Baseline vs. LP-PIESC. Average energy output with baseline optimal blade pitch angle and LP-PIESC (top), percentage change in energy capture (bottom).

The results suggest that the LP-PIESC gives an energy output very close to the baseline controller, where the optimal tuning parameter (blade pitch angle) value is known. The maximum energy loss was 0.5% (reduction of around 25 kWh) which was seen for the high wind speed of 12 m/s (15% TI). Averaging results across all wind conditions, we obtain Table 7.

Table 7. Average energy capture for LP-PIESC compared to baseline

	Baseline (kWh)	LP-PIESC (kWh)	% Change
Average Energy Output	2178.6	2172.6	−0.3

Table 7 suggests that due to the faster convergence of the blade pitch angle to its optimal value, the LP-PIESC could produce nearly optimal energy output. That is, the LP-PIESC could reach very close to the maximum energy output without knowing the optimal pitch angle setting. This optimal setting in the baseline controller could change over time due to the wear and tear of the blade surface, and variations in atmospheric and environmental conditions such as icing, insects, etc. Thus, whenever the current pitch angle is no longer optimal, the LP-PIESC can find the new optimal blade pitch angle without any significant loss in energy capture.

4.4. Structural Loads Analysis

This section shows the change in loads (blades, tower, drive train) due to the change in blade pitch angle imparted by the LP-PIESC. We investigate the impact on transient loads caused by the sudden change in the blade pitch angle as well as the effect of the dither signal on the wind turbine loads. The loads considered are shown in Table 5.

The LP-PIESC is evaluated for the hub-height mean wind speeds of 4 m/s, 8 m/s, and 12 m/s, no wind shear, and turbulence intensities (TI) of 10% and 15%, respectively. TurbSim [15] is used to generate wind profiles from six distinct seeds for each turbulent intensity case. The time series of the loads are analyzed with MLife to calculate aggregate damage equivalent loads (DELs) [19]. The DELs obtained from the time series of the LP-PIESC are then compared against those obtained from the baseline controller, i.e., $\beta = 0^\circ$. All the evaluations are done on the data from 150 s till the simulation end time of 3000 s. As shown in Figures 25 and 26, when the LP-PIESC is turned on, there is a sudden change in the blade pitch angle from the initial setting to the optimal value. This sudden change will propagate to a sudden change in the blade-root flap-wise bending moment (BRFW). Figure 28 illustrates this situation for the wind speeds shown in Figure 6.

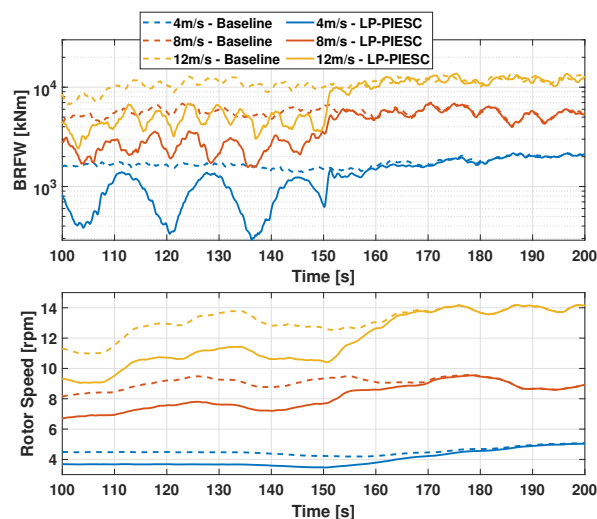


Figure 28. Effect of sudden change in blade pitch angle with LP-PIESC on blade-root flap-wise bending moment (BRFW) (**top**) and rotor speed (**bottom**) compared with the baseline (for hub height wind from Figure 6).

The response of the baseline constant blade pitch angle is shown as well. As expected, the BRFW and the rotor angular speed converges to the optimal time series, eventually.

4.4.1. Blade Loads

The first turbine component affected by the sudden change in the blade pitch angle should be the blades. For each wind condition, we calculate the average DEL over all three blades. The average DEL for the blade-root flapwise bending moment (BRFW) is shown in Figure 29.

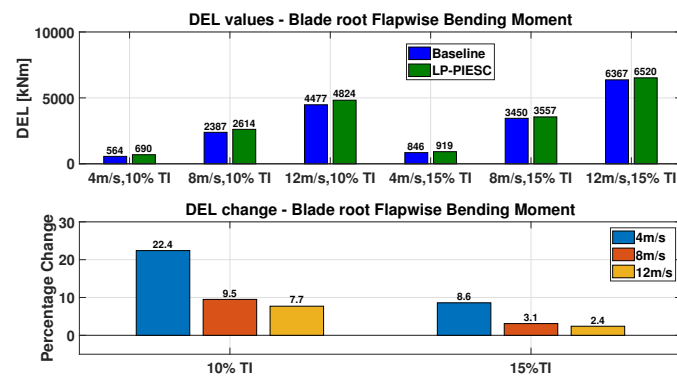


Figure 29. Blade root flap-wise bending moment comparison: Baseline vs. LP-PIESC. Aggregate DEL values with baseline controller and LP-PIESC (top), percentage change in DEL (bottom) for time series from 150 s to 3000 s.

Using LP-PIESC, the BRFW DELs increase for all wind conditions compared to the baseline controller. This increase can be attributed to the sudden change in the blade pitch angle (from sub-optimal to optimal), which leads to the sudden change in the BRFW as shown in Figure 28. From Figure 29, we can conclude that the percentage DEL change decreases with the increase in mean wind speed or the increase in turbulence intensity. The average increase across the three wind speeds ranges from 13% (10% TI) to 5% (15% TI). This could be because, at higher turbulence, fluctuations due to the wind could be relatively more significant than the effect of a step change in the blade pitch angle. The highest percentage change for both the 10% TI and 15% TI wind can be observed at the low wind speed case of 4 m/s which is likely due to the small actual DEL values.

We also calculated BRFW DELs for the time series from 300 s (once the transients die out) till the simulation end time (3000 s). The results are shown in Figure 30. Now, the average change in BRFW DELs is just 0.3% (10% TI) and 0.4% (15% TI). Thus, the DEL values with the LP-PIESC are essentially identical to those with the baseline controller. Furthermore, the presence of the continuous dither signal in the LP-PIESC does not affect the BRFW DELs.

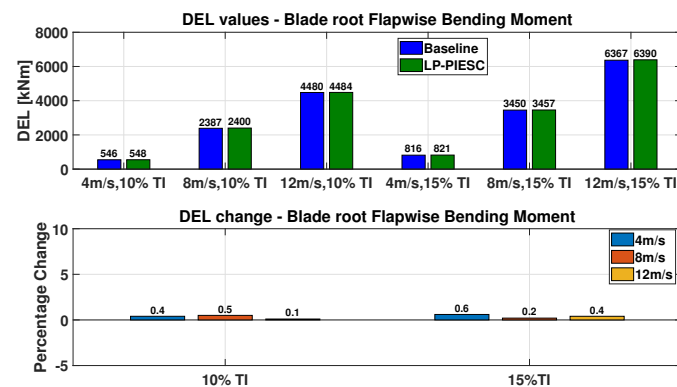


Figure 30. Blade root flap-wise bending moment comparison: Baseline vs. LP-PIESC. Aggregate DEL values with baseline controller and LP-PIESC (top), percentage change in DEL (bottom) for time series from 300 s to 3000 s.

DEL results for the blade-root edgewise moment (BREW) are shown in Figure 31. BREW does not show any change, i.e., the sudden change in the blade pitch angle or the dither signal of LP-PIESC does not affect the BREW.

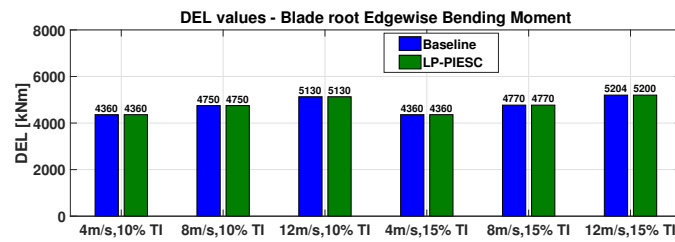


Figure 31. Blade root edge-wise bending moment comparison: Baseline vs. LP-PIESC. Aggregate DEL values with baseline controller and LP-PIESC for time series from 150 s to 3000 s.

4.4.2. Tower Loads

The tower-base fore-aft bending moment (TBFA) and tower-base side-side bending moment (TBSS) are evaluated. DEL results for the tower loads are shown in Figures 32 and 33.

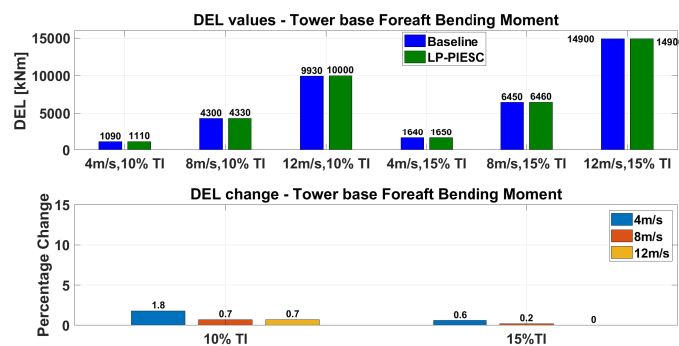


Figure 32. Tower base fore-aft bending moment comparison: Baseline vs. LP-PIESC. Aggregate DEL values with baseline controller and LP-PIESC (top), percentage change in DEL (bottom) for time series from 150 s to 3000 s.

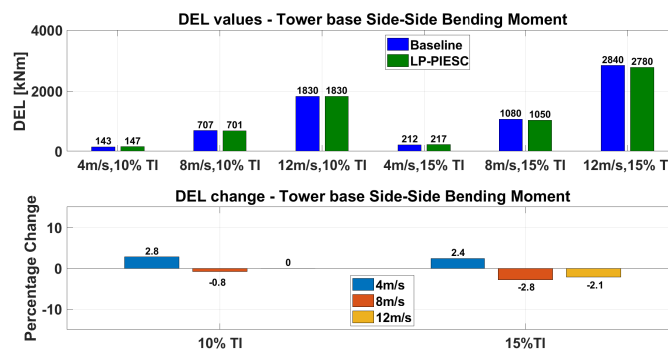


Figure 33. Tower base side-side bending moment comparison: Baseline vs. LP-PIESC. Aggregate DEL values with baseline controller and LP-PIESC (top), percentage change in DEL (bottom) for time series from 150 s to 3000 s.

For both the TBFA and TBSS, there is no substantial change in DELs, which means tower loads are not affected by the LP-PIESC.

4.4.3. Drivetrain Loads

We also evaluated the drivetrain torsion for both the LP-PIESC and the baseline controller. DEL results for drivetrain torsion are shown in Figure 34.

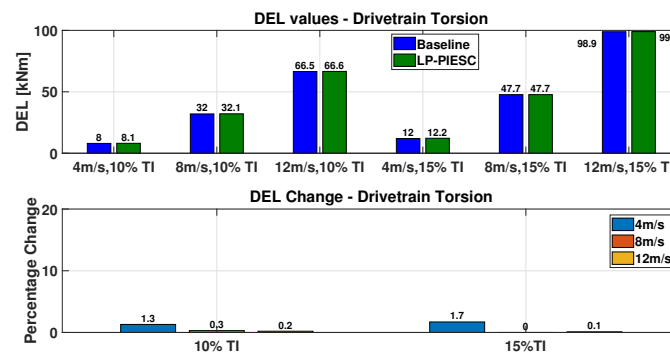


Figure 34. Drivetrain torsion comparison: Baseline vs. LP-PIESC. Aggregate DEL values with baseline controller and LP-PIESC (top), percentage change in DEL (bottom) for time series from 150 s to 3000 s.

Similar to the tower loads, drivetrain torsion is not affected by either the sudden change in blade pitch angle or the dither signal of the LP-PIESC for all the wind conditions. The average percentage change at both 10% TI and 15% TI wind is 0.6%.

5. Conclusions

This paper presented a log-power feedback PIESC (LP-PIESC) strategy for wind turbine power maximization in region-2. The proposed algorithm is compared with a conventional ESC with log-of-power feedback (LP-ESC) scheme. The performance of both strategies is evaluated using the NREL 5MW reference turbine model in OpenFAST. Simulations were performed under different below-rated wind conditions. The major improvements of the LP-PIESC, over the conventional LP-ESC, are

- (i) faster convergence to optimal parameters, and
- (ii) smaller dither amplitude to estimate the gradient of log-of-power with respect to the control parameters.

These initial results provide evidence supporting the hypothesis that the amalgamation of log-power feedback and PIESC technique could result in faster and consistent convergence across different below-rated wind speed conditions.

Design of the PIESC algorithm requires tuning more parameters than the conventional ESC. Additional work is needed to establish practical guidelines for parameter design customized to control of wind turbines and wind farms. In addition, evaluation of the LP-PIESC performance under wind conditions such as ramps or gusts should be performed to evaluate potential risks of this algorithm.

Author Contributions: D.K. contributed the LP-ESC and LP-PIESC design, simulations, analysis of results, and technical writing. M.A.R. defined the research direction and evaluation criteria for algorithm comparison, contributed to analysis of results and technical writing. All authors have read and agreed to the published version of the manuscript.

Funding: The authors acknowledge the support from the Center for Wind Energy at UT Dallas (UTD Wind).

Institutional Review Board Statement: Not applicable.

Informed Consent Statement: Not applicable.

Data Availability Statement: Not applicable.

Conflicts of Interest: The authors declare no conflict of interest.

Abbreviations

ESC	Extremum Seeking Control
LP-ESC	Log-of-Power Extremum Seeking Control
LP-PIESC	Log-of-Power Proportional-Integral Extremum Seeking Control
BRFW	Blade-Root Flapwise bending moment
BREW	Blade-Root Edgewise bending moment
TBFA	Tower-Base Fore-aft bending moment
TBSS	Tower-Base Side-side bending moment
DTT	Drivetrain Torsion
DEL	Damage Equivalent Load
NREL	National Renewable Energy Laboratory
TI	Turbulence Intensity

References

- Pao, L.Y.; Johnson, K.E. Control of Wind Turbines. *IEEE Control Syst.* **2011**, *31*, 44–62.
- Jonkman, J.; Butterfield, S.; Musial, W.; Scott, G. *Definition of a 5-MW Reference Wind Turbine for Offshore System Development*; Technical Report; National Renewable Energy Lab. (NREL): Golden, CO, USA, 2009.
- Creaby, J.; Li, Y.; Seem, J.E. Maximizing Wind Turbine Energy Capture Using Multivariable Extremum Seeking Control. *Wind Eng.* **2009**, *33*, 361–387. [[CrossRef](#)]
- Xiao, Y.; Li, Y.; Rotea, M.A. CART3 Field Tests for Wind Turbine Region-2 Operation With Extremum Seeking Controllers. *IEEE Trans. Control Syst. Technol.* **2019**, *27*, 1744–1752. [[CrossRef](#)]
- Rotea, M.A. Logarithmic Power Feedback for Extremum Seeking Control of Wind Turbines. *IFAC-PapersOnLine* **2017**, *50*, 4504–4509. [[CrossRef](#)]
- Ciri, U.; Leonardi, S.; Rotea, M.A. Evaluation of log-of-power extremum seeking control for wind turbines using large eddy simulations. *Wind Energy* **2019**, *22*, 992–1002. [[CrossRef](#)]
- Guay, M.; Dochain, D. A proportional-integral extremum-seeking controller design technique. *Automatica* **2017**, *77*, 61–67. [[CrossRef](#)]
- Kumar, D.; Rotea, M.A. Log-power PIESC for wind turbine power maximization below-rated wind conditions. In Proceedings of the AIAA Scitech 2021 Forum, Virtual Event, 11–15, 19–21 January 2021; Number AIAA 2021-1288; pp. 1–10. Available online: <https://arc.aiaa.org/doi/pdf/10.2514/6.2021-1288> (accessed on 18 December 2021).
- Rotea, M.A. Method and System for Using Logarithm of Power Feedback for Extremum Seeking Control. U.S. Patent Application 16/617,911, 2020.
- Krstic, M.; Kokotovic, P.V.; Kanellakopoulos, I. *Nonlinear and Adaptive Control Design*, 1st ed.; John Wiley & Sons, Inc.: Hoboken, NJ, USA, 1995.
- Adetola, V.; Guay, M. Robust adaptive MPC for constrained uncertain nonlinear systems. *Int. J. Adapt. Control Signal Process.* **2011**, *25*, 155–167. [[CrossRef](#)]
- Jonkman, J. The New Modularization Framework for the FAST Wind Turbine CAE Tool. In Proceedings of the 51st AIAA Aerospace Sciences Meeting including the New Horizons Forum and Aerospace Exposition, Grapevine, TX, USA, 7–10 January 2013; Number AIAA 2013-0202; pp. 1–26.
- Ariyur, K.B.; Krstic, M. *Real-Time Optimization by Extremum-Seeking Control*; John Wiley & Sons: Hoboken, NJ, USA, 2003.
- Rotea, M.A. Analysis of multivariable extremum seeking algorithms. In Proceedings of the 2000 American Control Conference. ACC (IEEE Cat. No.00CH36334), Chicago, IL, USA, 28–30 June 2000; Volume 1, pp. 433–437.
- Jonkman, B.J. *TurbSim User's Guide: Version 1.50*; Technical Report; National Renewable Energy Lab. (NREL): Golden, CO, USA, 2009.
- IEC. *Wind Energy Generation Systems—Part 1: Design Requirements*; IEC: Geneva, Switzerland, 2005.
- IEC. *Wind Energy Generation Systems—Part 1: Design Requirements*; International Electrotechnical Commission: Geneva, Switzerland, 2019.
- Jonkman, J.M.; Jonkman, B.J. FAST modularization framework for wind turbine simulation: Full-system linearization. *J. Phys. Conf. Ser.* **2016**, *753*, 082010. [[CrossRef](#)]
- Hayman, G.; Buhl, M., Jr. *Mlife Users Guide for Version 1.00*; Technical Report; National Renewable Energy Laboratory: Golden, CO, USA, 2012.